Research Article

Muhammad Tahir, Wafa Mohammed Almalki, Nasir Rahman, Mudasser Husain*, Mohamed Hussien, Vineet Tirth, Khamael M. Abualnaja, Abid Ali Khan, Amir Ullah, Rajwali Khan, and Aurangzeb Khan*

Physical properties of ternary chloro-perovskites $KTCl_3$ (T = Ge, Al) for optoelectronic applications

https://doi.org/10.1515/phys-2025-0217 received April 16, 2025; accepted July 18, 2025

Abstract: This study uses density functional theory to investigate various properties of ternary chloro-perovskites, KTCl₃ (T = Ge or Al). Both compounds have a cubic structure with lattice parameters of 5.159 Å for KAlCl₃ and 5.378 Å for KGeCl₃. KGeCl₃ has a direct band gap of 1.88 eV, while KAlCl₃ exhibits metallic behavior due to aluminum states crossing the energy level, indicating the material's ability to conduct electricity. Analysis of the electronic structure shows that the electronic properties of KGeCl₃ are primarily influenced by the interactions of germanium and chlorine orbitals, while those of KAlCl₃ are dominated by aluminum orbitals. Optical properties reveal that these materials exhibit strong absorption and high reflectivity in

the ultraviolet and visible light range. These properties suggest potential use in optoelectronic applications. Their mechanical stability is supported by elastic constant analysis, which shows their ductile nature and anisotropic behavior, as indicated by the bulk modulus, shear modulus, Young's modulus, and Poisson's ratio. Pugh's ratio values of 2.2711 and 2.5035 for KAlCl₃ and KGeCl₃, respectively, confirm ductility, while Poisson's ratio suggests a dominant ionic bonding character. These findings provide significant information on the material's potential applications.

Keywords: structural, elastic, and optoelectronic properties, DFT, Wien2K

1 Introduction

Perovskites ABX3, in which X is an anion and A and B are two cations, can result from arranging atoms in a variety of ways. This is because most elements in the periodic table have the ability to exchange for ones in the A and B locations. Six X anions coordinate with the B-site cations, which are located in the center of the octahedron in a unit cell. while A cations are located in the upper corner of the cube [1,2]. Researchers have conducted a significant amount of research on the ABX₃ perovskites due to their enormous number of structural families with specific properties, which have allowed them to find substantial roles in various potential applications [3,4]. Recently, halide perovskite from I–IV–VII materials has shown amazing results for their expected applications as a photocatalytic cell absorber, as insulating materials, and semiconducting behavior. Cheng et al. investigated a new variety of all-solid-state and inorganic photocatalytic cell system that comprises the P-type direct band gap semiconducting CsSnI₃ with n-type TiO₂ with N719 dye, exhibiting a variant ratio of up to 11.3%. Similarly, Lee et al. investigated an inexpensive solution based on solar cells, which depends on an extremely crystalline absorbing material (CH₃NH₃PbI₂Cl) with high-frequency light or equal to infrared absorptivity, which has a more

e-mail: akhan@awkum.edu.pk

Muhammad Tahir: Department of Physics, Abdul Wali Khan University, Mardan, 23200, Pakistan

Wafa Mohammed Almalki: Department of Physics, Turabah University College, Taif University, P.O. Box 11099, Taif, 21944, Saudi Arabia Nasir Rahman: Department of Physics, University of Lakki Marwat, Lakki Marwat, KPK, 28420, Pakistan, e-mail: nasir@ulm.edu.pk

Mohamed Hussien: Department of Chemistry, Faculty of Science, King Khalid University, P.O. Box 9004, Abha, 61413, Saudi Arabia, e-mail: mhalmosylhy@kku.edu.sa

Vineet Tirth: Mechanical Engineering Department, College of Engineering, King Khalid University, Abha, Aseer, 61421, Saudi Arabia; Centre for Engineering and Technology Innovations, King Khalid University, Abha, Aseer, 61421, Saudi Arabia, e-mail: vtirth@kku.edu.sa Khamael M. Abualnaja: Department of Chemistry, College of Science, Taif University, Taif, 21944, Saudi Arabia

Abid Ali Khan: Department of Chemical Sciences, University of Lakki Marwat, Lakki Marwat, KPK, 28420, Pakistan

Amir Ullah: Department of Chemistry, Hazara University, Mansehra, KPK, Pakistan

Rajwali Khan: National Water and Energy Center, United Arab Emirates University, Al Ain, 15551, United Arab Emirates

^{*} Corresponding author: Mudasser Husain, State Key Laboratory of Mesoscopic Physics and Department of Physics, Peking University, Beijing, 100871, China, e-mail: 2201110247@stu.pku.edu.cn

^{*} Corresponding author: Aurangzeb Khan, Department of Physics, Abdul Wali Khan University, Mardan, 23200, Pakistan,

power efficiency of 11.9% in a single cell device in full sunlight [5]. Recently, Bursschka et al. prepared solar cells based on CH₃NH₃PbI₃/TiO₃ with a power conversion efficiency of up to 15% and high stability gain. Daniel et al. studied LiBaF₃ and reported that such types of compounds are good for energy storing devices. All the newly conducted experiments showed that such types of materials are important for solar cells as absorbing materials. Yet, theoretical reports on this type of material were quite incomplete. Borriello et al. reported the structural and electronic properties of tin-based ABX3 compounds. Murtaza and Ahmad studied the structural and optoelectronic properties of cubic perovskites $CsPbX_3$ (X = Cl, Br, I) [6]. Cheng et al. also studied the electronic and structural properties of lead-based ABX₃ compounds. Recently, Mosconi et al. studied the different aspects of CH₃NH₃PbX₃ and mixed halide perovskites. Ternary halides have been the perovskite crystal of interest for some time now because of their expanding applications in the electrical, magnetic, and superionic domains [7,8]. It has recently been discovered that CsPbI3 and CsPbBr3 metal halides exhibit excellent photo, thermal, and moisture-resistant properties. Long-term stability of the perovskite structural alloy MAPbBr3 was obtained by Kulbak et al. by substituting the organic MA⁺ cation with Cs to generate CsPbBr₃. In recent years, significant advancements have been made in the study of chloro-perovskites for optoelectronic applications. Recent studies have explored the structural, electronic, and optical properties of various chloro-perovskite compounds, highlighting their potential for high-efficiency solar cells, photodetectors, and other optoelectronic devices [9-11]. Our study aims to contribute to this growing body of research by investigating the properties of KTCl₃ (T = Ge, Al) and comparing them with state-ofthe-art materials to highlight their unique advantages and potential applications. In this study, we report a broad study of the structural, electronic, optical, and elastic properties of the cubic perovskites KTCl₃ (T = Ge or Al) using the FP-LAPW approach based on density functional theory (DFT). We also report the optical properties of these materials, which are best for photocatalytic cells with a perfect absorber with good optical absorption [12,13].

2 Computational methodology

In this study, first-principles calculations using the FP-LAPW method are implemented in the WEIN2k code based on DFT. In this method, the augmented plane wave and the solution to the KohnSham equation are performed self-consistently, and a local orbital basis set is organized to

show the electronic band structure for all atoms and their related orbitals. All the calculations were converged with respect to the size of the basis set and Brillouin zone (BZ) sampling [14,15]. A tetrahedron technique is used to determine the BZ integration within the self-consistency cycle performance. The correlation and exchange effects treated within the three potentials are the modified BeckeJohnson exchange potential (mBJ) and gradient approximation (GGA) based on the FP-LAPW method [16,17]. Many DFT scientists used this technique. The k-mesh points used in the BZ are $20 \times 20 \times 20$ for a well-conserved self-consistency cycle. The energy cut-off is set to 10⁻⁵ Rv. as suggested previously [18]. The convergence parameter $R_{\rm MT}K_{\rm max}$, which controls the size of the basis sets, is set to 7, which indicates convergence, where K_{max} is the plane wave cutoff and $R_{\rm MT}$ is the smallest of all the atomic sphere radii. The $G_{\rm max}$ parameter was selected to be 12 a.u⁻¹.

3 Results and discussion

3.1 Structural properties

KTCl₃ (T = Ge or Al) has a cubic perovskite structure described by the formula ABCl₃, as displayed in Figure 1. Potassium (K) is at the A-site, while aluminum (Al) or germanium (Ge) is at the B-site. In both compounds, K is located at (0, 0, 0), and Cl is located at (0.5, 0.5, 0.5). Al and Ge share the same (0.5, 0.5, 0.5) position (Table 1). Both compounds have the same Pm3-m (221) space group, indicating a cubic unit cell arrangement [19–22]. The elemental configuration for atoms is K: $(1s^2, 2s^2, 2p^6, 3s^2, 3p^6, 3d^1)$, Cl: $(1s^2, 2s^2, 2p^6, 3s^2, 3p^5)$, Al: $(1s^2, 2s^2, 2p^6, 3s^2, 2p^1)$, and Ge: $(1s^2, 2s^2, 2p^6, 3s^2, 3p^6, 3d^{10}, 4s^2, 4p^2)$.

Table 2 shows the calculated properties used to assess the structural stability of $KTCl_3$ (T = Ge or Al), such as

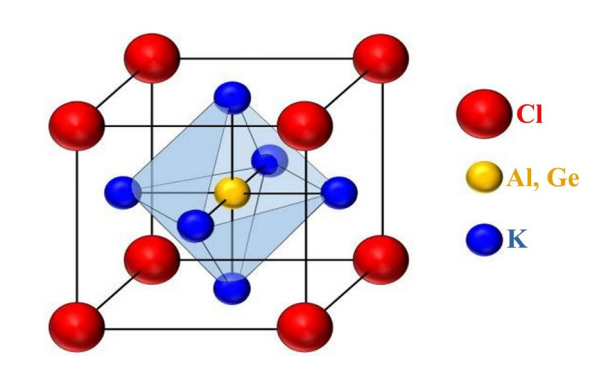


Figure 1: Crystal structure of KTCl₃ (T = Ge or Al) perovskites.

Table 1: Unit cell structural parameters of KTCl₃ (T = Ge or Al)

Atoms	Coordination number	Wyckoff position	Multiplicity	Symmetry	Coordinates
A (K)	12	a	1	m-3m	(0.0, 0.0, 0.0)
B (Al/Ge)	6	b	1	m-3m	(0.5, 0.5, 0.5)
X (CI)	2	С	4	4/m m.m	(0.5, 0.0, 0.5)
					(0.5, 0.0, 0.5)
					(0.5, 0.0, 0.5)

Table 2: Data computed from optimized crystal unit cells of KTCl₃ (T = Ge or Al) perovskites

Crystals	Lattice constant (a_0) (Å)	Bulk modulus (<i>B</i>) (GPa)	Bulk modulus derivative (<i>B'</i>)	Equilibrium volume (V_0) (a.u. ³)	Ground-state energy (E_0) (Ry)
KGeCl ₃	5.378	27.3900	5.0000	996.41	-8171.90
KAICI ₃	5.159	31.5846	5.0000	891.71	-4459.40

lattice constant (a_0) , bulk modulus (B), bulk modulus pressure derivative (B'), equilibrium volume (V_0), and groundstate energy (E_0) . KGeCl₃ has a larger lattice constant (a_0) of 5.378 Å, a smaller bulk modulus (B) of 27.3900 GPa, and an equilibrium volume (V_0) of 996.41 a.u.³ KAlCl₃ has a smaller lattice constant (a_0) of 5.159 Å, a larger bulk modulus (B) of 31.5846 GPa, and an equilibrium volume (V_0) of 891.71 a.u.³, as shown in Table 2. The bulk modulus pressure derivative (B') is the same for both compounds at 5.0000. The groundstate energy (E_0) is lower for KAlCl₃ (-4459.40 Ry) compared to KGeCl₃ (-8171.90 Ry) (Figure 2).

The ability of a material to resist compression, known as its bulk modulus (B), is higher for KAlCl₃ (31.5846 GPa) compared to KGeCl₃ (27.3900 GPa). This indicates that KAlCl₃ is mechanically more rigid and less prone to compression. Furthermore, the bulk modulus pressure

derivative (B') for both compounds is similar (5.0000), which aligns with typical values for chloro-perovskites. This similarity suggests that both compounds exhibit stability under low-pressure conditions [23,24].

The most stable electronic arrangement for KGeCl₃ (ground-state energy: -8171.90 Ry) requires less energy than that of KAlCl₃ (-4459.40 Ry). This difference indicates that KGeCl₃ has a more stable electronic structure and is easier to form. The lower formation energy of KGeCl3 suggests that it is structurally less dense and more mechanically flexible than KAlCl₃. In summary, KGeCl₃ has a lower formation energy, making it a softer material, while KAlCl₃ is structurally denser and more rigid. These differences affect their potential applications, with KGeCl₃ being more suitable for electronic and optoelectronic uses due to its lower formation energy and better adaptability [25-27].

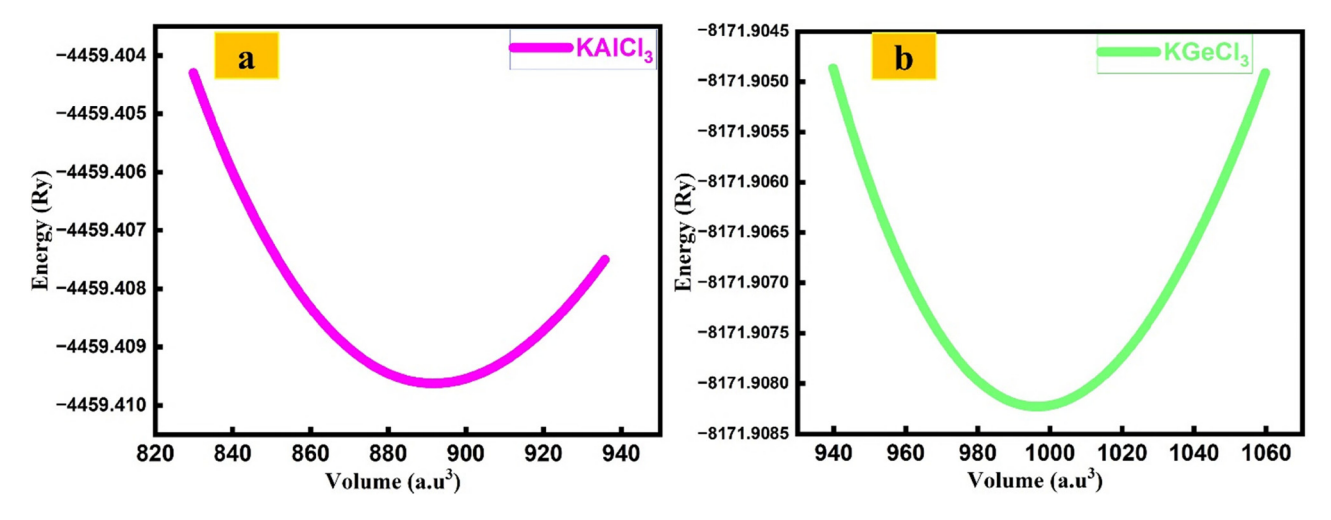


Figure 2: Optimization curve of KTCl₃ (T = Ge or Al) perovskites. : (a) KAlCl₃ and (b) KGeCl₃.

3.2 Electronic properties

The electronic properties of KTCl₃ (T = Ge or Al) differ significantly. KGeCl₃ has a direct band gap of 1.88 eV, meaning it can effectively convert light into electricity (Figure 3). This property makes it a good choice for optoelectronic devices like solar cells, photodetectors, and lights. The direct band gap allows for efficient movement of electrons between different energy levels, enhancing its ability to generate or emit light. The analysis of the density of available energy states (DOS) shows that potassium (K) slightly affects the valence band, with minor contributions from specific energy states, as shown in Figure 4. Germanium (Ge), on the other hand, significantly influences both the valence and conduction bands. Ge contributes to the valence band with one type of energy state, while it has a prominent contribution to the conduction band with a different type of state. This indicates Ge's importance in the material's ability to conduct charge. Chlorine (Cl) makes its presence felt primarily in the valence band, with two types of states dominating. In contrast, a different Cl state plays a significant role in the conduction band, highlighting its influence on electronic transitions. The substantial contributions from both Ge and Cl orbitals underscore KGeCl₃'s effectiveness as a semiconductor material.

In contrast, KAlCl₃ has no band gap, making it an excellent electrical conductor (Figure 3). This property is ideal for electronics applications, such as interconnects and charge transport layers. The analysis of the density of states (DOS) reveals that potassium (K) contributes significantly to the valence band, primarily through the K (red) state, with additional contributions from K-d (yellow) and K-f (brown) states, as displayed in Figure 4. Aluminum (Al) plays a crucial role in conductivity, with its blue electronic state crossing the Fermi level. This direct connection between the valence and conduction bands forms a peak in the conduction band, confirming the metallic nature of KAlCl₃. Additionally, the Al-p (cyan) state contributes to the metallic character. The element chlorine (Cl) plays a crucial role in the energy band structure of the material KAlCl₃, influencing its electrical properties. Various Cl states contribute to the valence band, the energy range where electrons participate in electrical conduction. The Cl-green, Cl-p (violet), and Cl-d (green) states have a dominant presence in this band, while the Cl-f (orange) state is positioned slightly higher in energy. The presence of these chlorine states enhances the metallic characteristics of KAlCl₃, giving it excellent electrical conductivity. As a result, KAlCl₃ is well-suited for applications in conductive coatings, electrode materials, and electronics, where efficient charge transport is essential. KGeCl₃'s semiconductor properties make it suitable

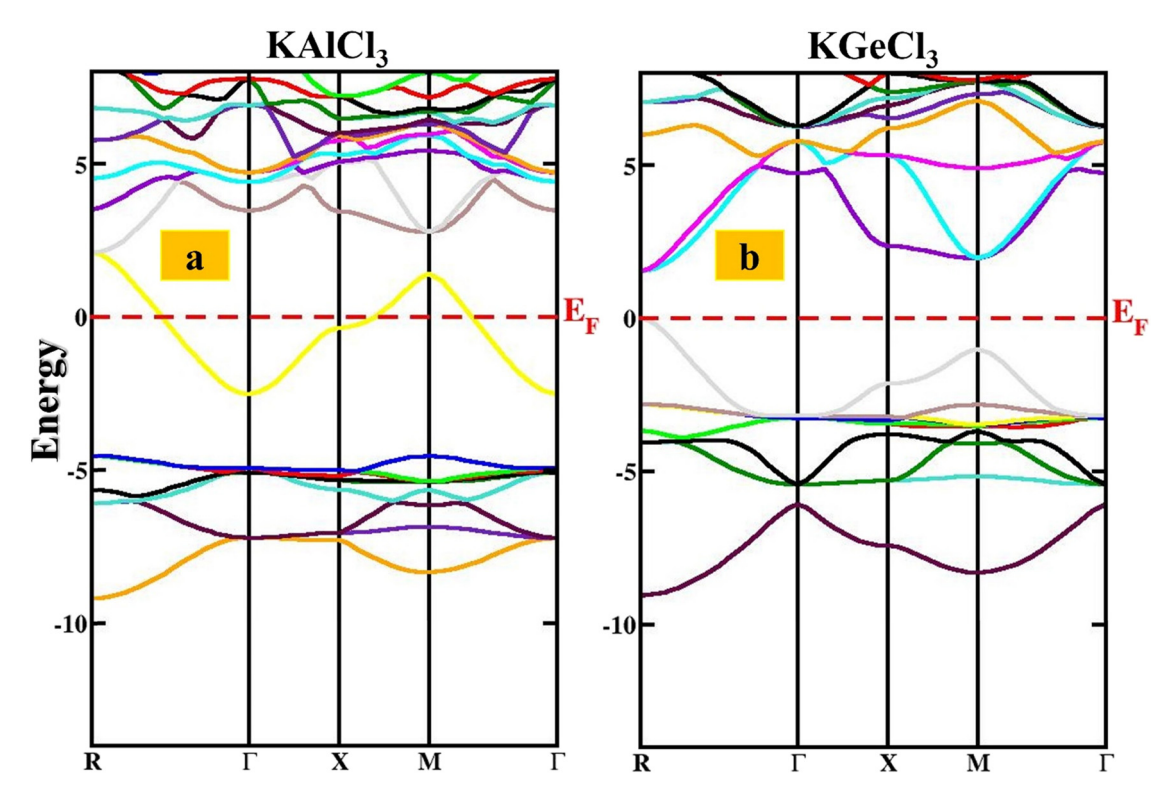


Figure 3: Electronic band structures of KTCl₃ (T = Ge, Al) perovskites: (a) KAlCl₃ and (b) KGeCl₃.

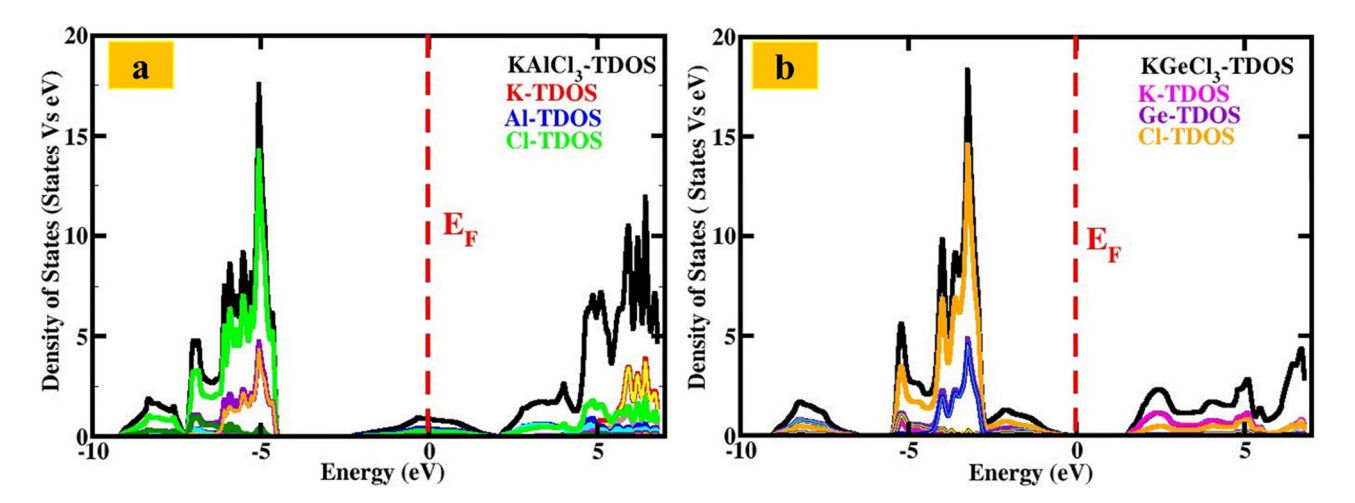


Figure 4: Total and partial density of states (DOS) versus energy for KTCl₃ (T = Ge, Al) perovskites: (a) KAlCl₃ and (b) KGeCl₃.

for optics and solar power due to its ability to conduct electricity only under specific conditions. On the other hand, KAlCl₃'s metallic properties make it a promising choice for coatings, circuits, and transporting electrical charges. KGeCl₃'s Ge and Cl atoms enable electron movement, making it ideal for devices that convert light into electricity. In contrast, KAlCl₃'s Al gives it high electrical conductivity, making it useful for electrical components and as a conductor. These properties make KTCl₃ (T = Ge or Al) crucial for developing advanced electronics and optical technologies.

3.2.1 Optical properties

3.2.1.1 Real and imaginary parts of the dielectric function

The dielectric response of KTCl₃ (T = Ge, Al) reveals their optical behavior, where ε_1 represents light refraction and ε_2 denotes absorption due to electronic transitions [28–33].

The optical response of potassium-based trichlorides, KAlCl₃ and KGeCl₃, is evaluated through their complex dielectric functions, offering insight into their suitability for optoelectronic applications. The real part of the dielectric function (ε_1) for KAlCl₃ exhibits an initial value of 3.30 at 3.25 eV, decreases to 2.91 at 6.33 eV, and increases to 3.25 at 9.51 eV, indicating moderate dispersion and wavelength-dependent refractive behavior. In comparison, KGeCl₃ demonstrates a significantly higher initial ε_1 of 4.92 at 2.06 eV, declining to 2.06 at 5.41 eV and increasing again to 3.34 at 9.82 eV, suggesting higher polarizability and enhanced refractive index attributes favorable for high-index optical components. The imaginary part of the dielectric function (ε_2), which describes photon absorption due to electronic transitions, further distinguishes the materials (Figure 5).

KAlCl₃ shows moderate absorption at 3.75 eV (ε_2 = 1.23), a pronounced UV absorption at 9.84 eV (ε_2 = 3.68), and a weaker peak at 12.10 eV (ε_2 = 3.01), signifying its applicability in UV photonics and filtering. Conversely, KGeCl₃ features a strong absorption peak in the near-UV region at 3.33 eV (ε_2 = 3.50), a dip at 5.75 eV (ε_2 = 2.48), followed by renewed absorption at 10.15 eV (ε_2 = 3.82), indicating robust interaction with a broader energy range. These findings highlight KGeCl3's potential for tunable photonic devices and high-refractive-index optics, while KAlCl₃ offers thermal and optical stability suitable for components such as capacitors, waveguides, and dielectric layers.

3.2.1.2 Optical conductivity and absorption coefficient

The electronic and optical behavior of $KTCl_3$ (T = Ge, Al) is governed by their conductivity and light absorption characteristics [34–36].

KAlCl₃ demonstrates a notable increase in electrical conductivity with increasing photon energy, starting from a modest $668 \,\Omega^{-1} \, \text{cm}^{-1}$ at $3.74 \, \text{eV}$ and peaking at $5,007 \,\Omega^{-1} \, \mathrm{cm}^{-1}$ at $10.62 \, \mathrm{eV}$, as shown in Figure 6(a). This trend indicates strong photon-induced carrier excitation and enhanced charge transport under high-energy illumination. The conductivity remains elevated $(4,898 \,\Omega^{-1} \, \text{cm}^{-1})$ at 12.12 eV), suggesting its potential for integration into high-frequency optoelectronic devices, such as UV photodetectors and dielectric components in optical systems. In comparison, KGeCl₃ exhibits higher initial conductivity $(1.862 \,\Omega^{-1} \, \, \text{cm}^{-1} \, \, \text{at } \, 4.33 \, \text{eV})$ and peaks at $5.228 \,\Omega^{-1} \, \, \text{cm}^{-1}$ at 10.20 eV, with a slight decrease to $4,300 \,\Omega^{-1} \, \text{cm}^{-1}$ at 12.33 eV. These characteristics confirm its excellent charge mobility and suitability for high-speed and UV-range electronic applications.

6 — Muhammad Tahir et al. DE GRUYTER

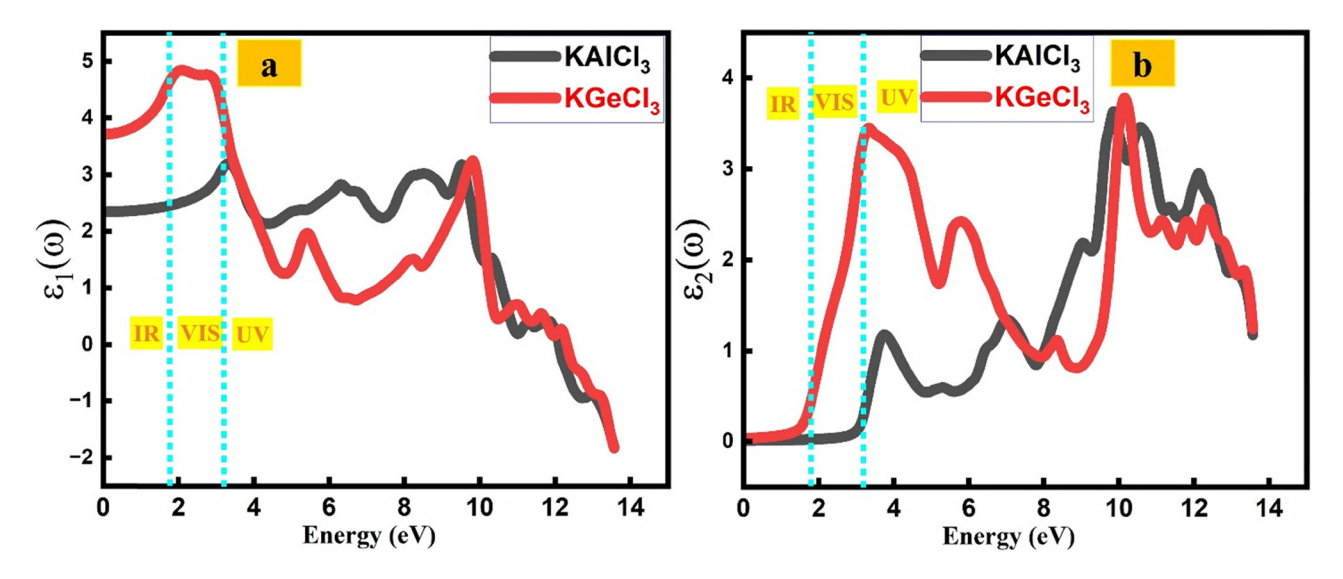


Figure 5: (a) Real part of the dielectric function of KTCl₃ (T = Ge or Al) perovskites. (b) Imaginary part of the dielectric function of KTCl₃ (T = Ge or Al) perovskites.

Optical absorption behavior, represented by the absorption coefficient in Figure 6(b), further distinguishes the two materials. KAlCl₃ shows significant absorption in the near-UV region, with a peak value of 16.95 at 3.78 eV, making it suitable for optical coatings and UV-sensitive materials. However, its absorption decreases at higher energies (1.34 at 10.87 eV and 1.97 at 13.60 eV), limiting its performance in the deep-UV range. In contrast, KGeCl₃ exhibits superior absorption across a broader energy spectrum, with values increasing from 45.81 (4.56 eV) to 125.60 (10.31 eV), reaching a maximum of 187.76 at 13.58 eV. This strong and sustained absorption indicates its potential for

high-performance UV photodetectors, protective coatings, and solar-energy-harvesting technologies.

3.2.1.3 Reflection and extinction coefficients

KTCl₃ (T = Ge, Al) shows promising photonic potential, as indicated by its reflection and extinction coefficients [28,37]. The extinction coefficient indicates how a material absorbs and scatters light, affecting transmission and energy loss in optical devices [38,39].

The optical reflectivity of $KTCl_3$ (T = Al, Ge) exhibits strong energy dependence, as illustrated in Figure 7(a). For

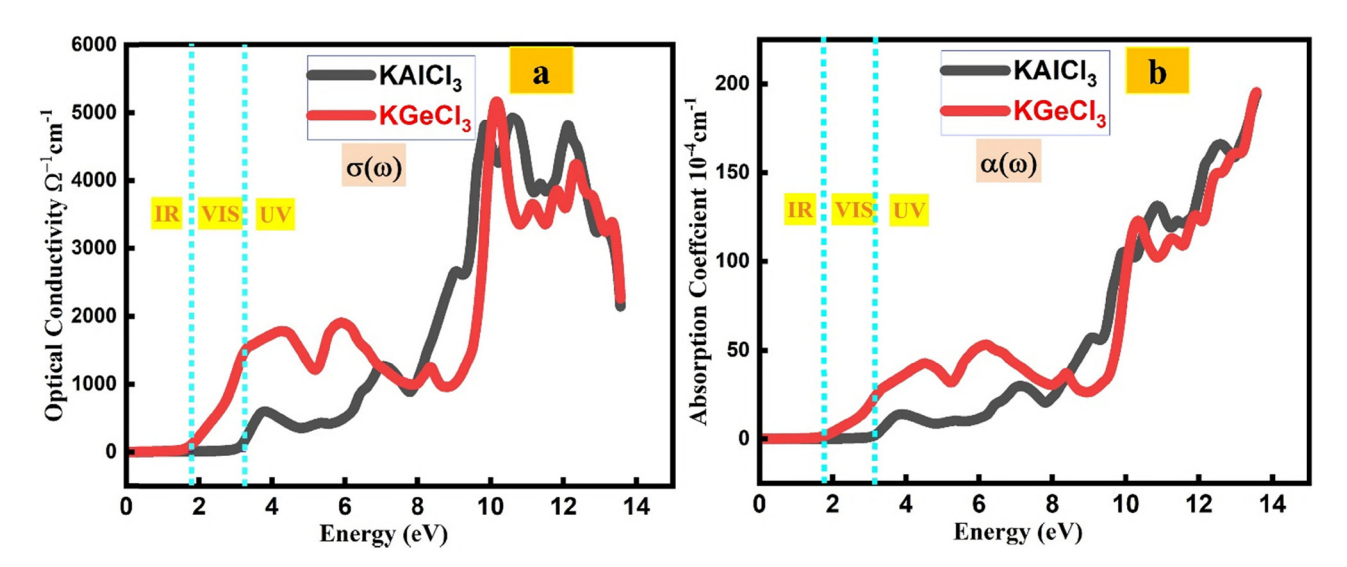


Figure 6: (a) Optical conductivity of KTCl₃ (T = Ge or Al). (b) Absorption coefficient of KTCl₃ (T = Ge or Al).

KAlCl₃, reflectivity is relatively low (9.6%) at 3.56 eV, enhancing its transparency in the lower energy range. However, it increases significantly with photon energy, reaching 23% at 10.90 eV and peaking at 60% around 13.58 eV, indicating potential for energy-selective optical coatings and antireflective applications. In contrast, KGeCl₃ demonstrates higher initial reflectivity (13.2% at 3.21 eV), with sustained moderate reflection across the spectrum and a sharp increase to 58% at 13.58 eV, making it suitable for high-reflectance mirrors and UV shielding in optoelectronic systems.

The extinction coefficient $\kappa(\omega)$, shown in Figure 7(b), quantifies a material's ability to attenuate light *via* absorption and scattering. For KAlCl₃, κ increases from 0.37 at 3.82 eV to 1.43 at 13.60 eV, indicating strong absorption in the highenergy UV region. KGeCl₃ shows consistently higher κ values across the same range, beginning at 0.95 (4.44 eV) and reaching 1.43 at 13.56 eV. Its broad and gradual increase suggests enhanced light attenuation, making KGeCl3 more effective for UV-blocking applications, optical filters, and light management components in photonic devices.

3.2.1.4 Refractive index and energy loss function (ELF)

The refractive index and ELF of $KTCl_3$ (T = Ge, Al) indicate their light-bending and energy-loss characteristics, essential for optical device design [34,37,40]. The ELF reflects energy loss from electron interactions, revealing plasmonic and dielectric behavior for advanced tech applications.

The refractive index $n(\omega)$ of KTCl₃ (T = Al, Ge), shown in Figure 8(a), reveals their light-bending capabilities across the photon energy spectrum. KAlCl₃ exhibits a maximum refractive index of ~1.83 at low energy (~2.62 eV), which gradually decreases with increasing energy, indicating normal dispersion behavior. KGeCl₃ shows a higher peak value of ~2.23 at 2.64 eV, suggesting stronger light confinement and enhanced optical density. These refractive characteristics make both compounds suitable for integrated photonic components such as lenses, waveguides, and optical coatings where precise light propagation is critical.

The energy loss function $ELF(\omega)$, plotted in Figure 8(b), quantifies the energy dissipated by fast electrons traversing the material, primarily associated with plasma resonance peaks. KAlCl₃ shows a prominent ELF peak at 12.65 eV, while KGeCl₃ exhibits its maximum around 13.12 eV, corresponding to bulk plasmon excitations. These peaks indicate strong electron-energy loss near these energies, critical for understanding dielectric screening and charge carrier dynamics. The distinct ELF profiles suggest potential applications in plasmonic devices, electron microscopy coatings, and highfrequency dielectric components.

3.3 Elastic properties

The elastic constants (C_{ii}) measure how a material reacts to stress, specifically its tendency to deform and recover its shape when stress is applied and removed. For cubic crystals like KTCl₃ (T = Ge or Al), three key constants (C_{11} , C_{12} , and C_{44}) govern their mechanical properties [41–43]. These constants are calculated using the Charpin method within the WIEN2K program. To ensure mechanical stability, the elastic constants must meet specific conditions: $(C_{11} - C_{12}) >$ 0, $(C_{11} + 2C_{12}) > 0$, and $C_{44} > 0$. Additionally, the condition

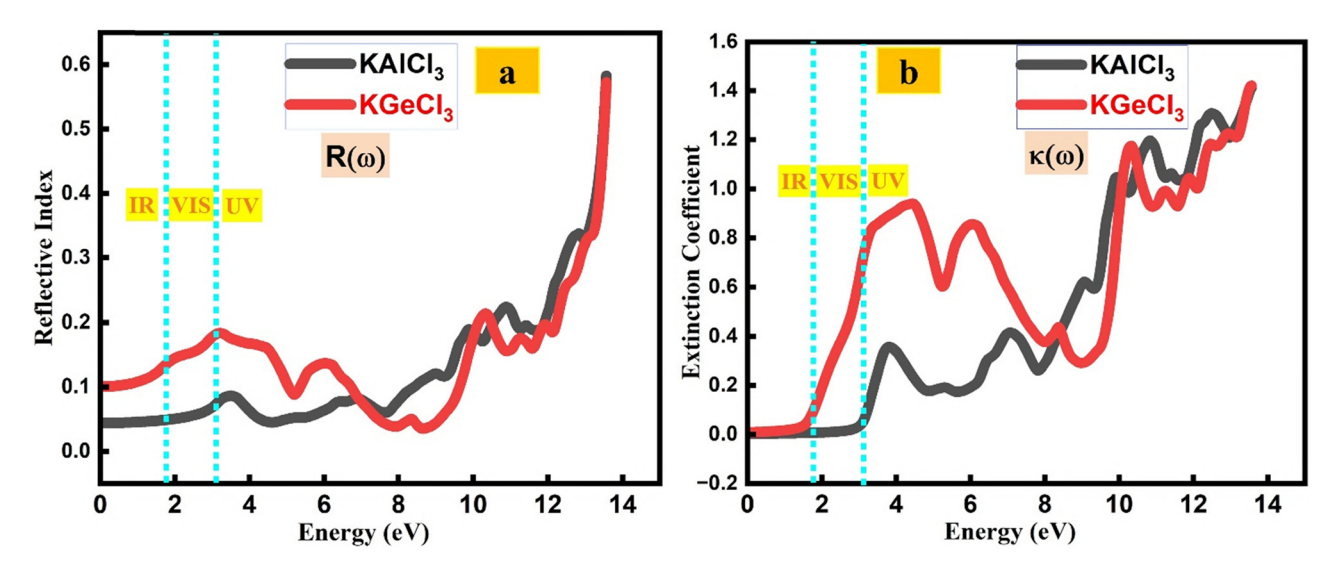


Figure 7: (a) Reflective index of KTCl₃ (T = Ge or Al). (b) Extinction coefficient of KTCl₃ (T = Ge or Al).

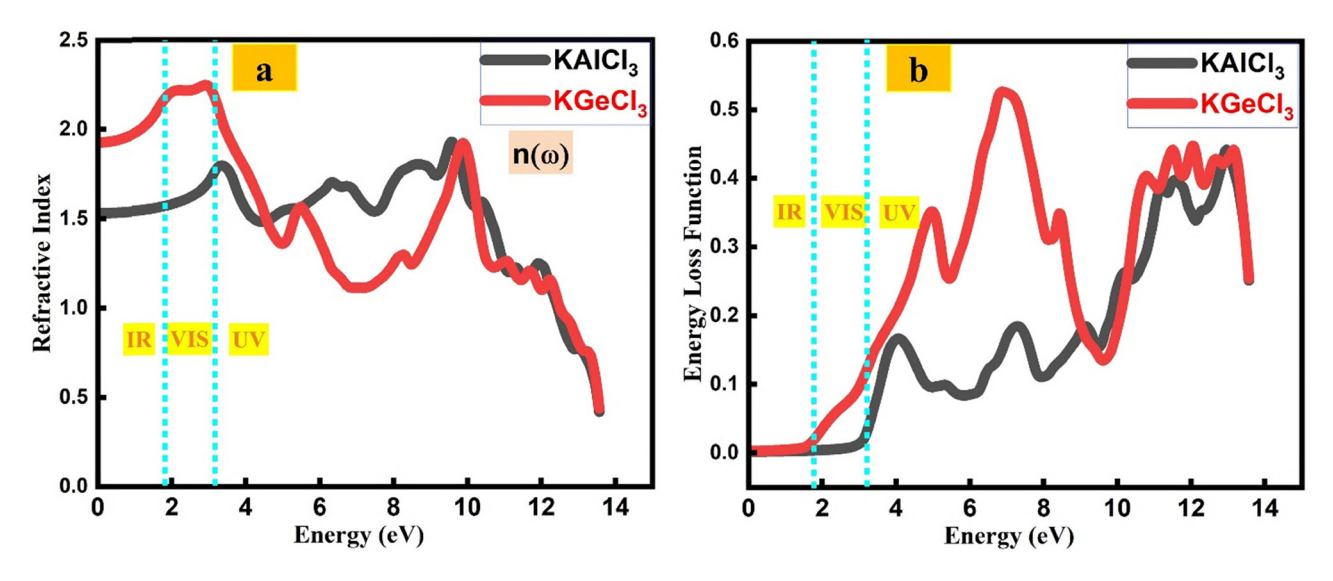


Figure 8: (a) Refractive index of KTCl₃ (T = Ge or Al). (b) ELF of KTCl₃ (T = Ge or Al).

 $C_{12} < B < C_{11}$ confirms the mechanical stability of these cubic compounds, where B is the bulk modulus. As there are no existing data on the elastic properties of $KTCl_3$ (T = Ge or Al), our calculated values can provide a reference for future research [31]. Using the following equations, we determined the mechanical parameters: anisotropy factor (A), shear modulus (G), Young's modulus (E), and Poisson's ratio (v):

$$A = \frac{2C44}{C11 - C44},\tag{1}$$

$$E = \frac{9GB}{3B + G'},\tag{2}$$

$$V = \frac{3B - 2G}{4B + 2G},\tag{3}$$

$$G = \frac{1}{2G_{\rm V} + 2G_{\rm R}},\tag{4}$$

$$G_{\rm Y} = \frac{1}{2C11 - 2C12 + 3C44},\tag{5}$$

$$G_{\rm R} = \frac{5C44(C11 - C12)}{4C44 + 3(C11 - C12)}.$$
 (6)

The shear modulus of the materials is represented by G [43], with G_r and G_v representing the lower and upper bounds, respectively. The anisotropy factor (A) measures

the material's departure from isotropy (A = 1) or indicates anisotropy ($A \neq 1$). Our results show that KAlCl₃ (A = 0.65) and KGeCl₃ (A = 0.36) are anisotropic, as indicated by their A values [44,45].

Young's modulus (E) measures material stiffness [46], with higher values indicating stiffer materials. Poisson's ratio (ν) gives insights into bonding characteristics. Values of ν below 0.1 indicate strong covalent bonding, while values around 0.25 suggest ionic character. Our calculations show ν as 0.56 for KAlCl $_3$ and 0.23 for KGeCl $_3$, suggesting both materials have significant ionic bonding contributions.

The Pugh's ratio (*B*/*G*) helps predict a material's behavior as ductile or brittle. Ductile behavior is indicated by a Pugh's ratio greater than 1.75. In the case of KAlCl₃ and KGeCl₃, their respective Pugh's ratios are 2.2711 and 2.5035, which both exceed the ductile threshold. This indicates that both compounds exhibit mechanical ductility [47] (Table 3).

The different ways KTCl₃ (T = Ge or Al) react to being stretched or squished (their elastic properties) give us a better understanding of how they move and remain stable. These properties vary depending on the direction of the force, as shown in detailed visualizations of their stiffness (Young's modulus), resistance to shearing (shear modulus), and tendency to change shape when stretched (Poisson's

Table 3: Elastic properties of KTCl₃ (T = Ge or Al)

Compound	C ₁₁ (GPa)	C ₁₂ (GPa)	C ₄₄ (GPa)	B (GPa)	А	<i>G</i> (GPa)	E (GPa)	Υ	B/G
KAICI ₃	35.1975	27.3021	19.32	80.65	0.65	35.51	210	0.56	2.2711
KGeCl₃	58.64	36.42	22.44	70.45	0.36	28.14	170	0.23	2.5035

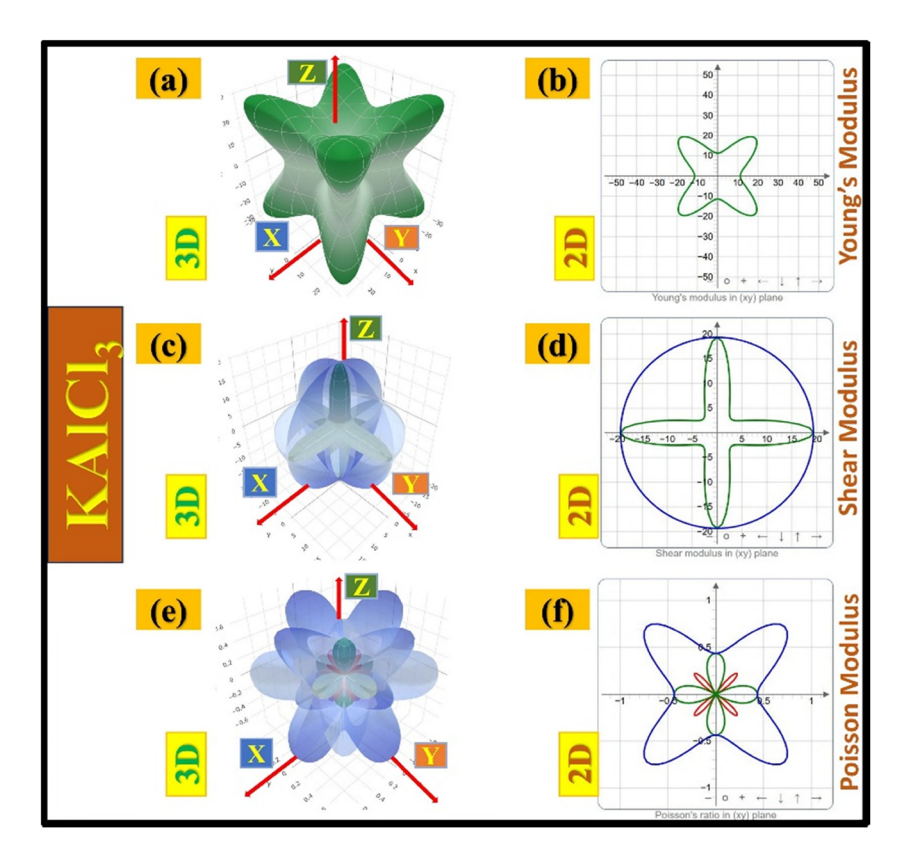


Figure 9: Anisotropic elastic properties of KAICl₃, illustrating variations in Young's modulus, shear modulus, and Poisson's ratio through 3D and 2D representations.

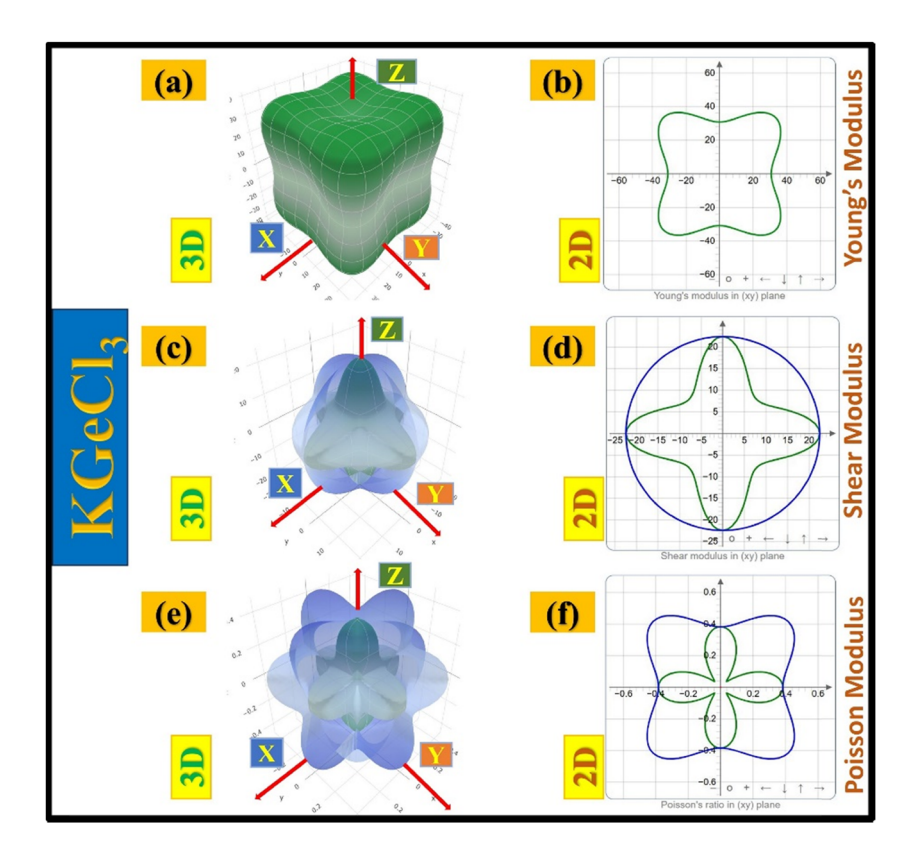


Figure 10: Anisotropic elastic properties of KGeCl₃, illustrating variations in Young's modulus, shear modulus, and Poisson's ratio through 3D and 2D representations.

10 — Muhammad Tahir et al. DE GRUYTER

Table 4: Comparative stud	y of KTCl ₃ (T = Ge, Al) with other compounds
---------------------------	------------------------------------	------------------------

Material	Band gap (eV)	Absorption coefficient (cm ⁻¹)	Bulk modulus (GPa)	Shear modulus (GPa)	Reference
KGeCl ₃	1.88	187.76	27.39	28.14	This study
KAICI₃	Metallic	16.95	31.58	35.51	This study
CsPbBr ₃	2.30	150.00	30.00	30.00	[48]
MAPbI ₃	1.56	120.00	25.00	20.00	[49]
CsGeCl ₃	1.80	160.00	28.00	29.00	[50]

ratio). KAlCl₃ exhibits highly variable stiffness in different directions, as seen in the star-shaped Young's modulus plot (Figure 9(a)). When force is applied, the material's response differs based on the direction. This asymmetry is also evident in the 2D projection (Figure 9(b)). Similarly, the shear modulus plots (Figure 9(c) and (d)) show varying resistance to deformation forces, indicating non-uniform deformation behavior. The Poisson's ratio plots (Figure 9(e) and (f)) further highlight this anisotropic behavior, indicating that KAlCl₃'s deformation pattern is strongly influenced by its crystal structure.

KGeCl₃ has a more symmetrical and cubic-like distribution of its Young's modulus in three dimensions (Figure 10(a)), indicating less anisotropy than KAlCl₃. Its 2D projection of Young's modulus (Figure 10(b)) shows less directional variation, suggesting a more balanced stiffness response in different crystal orientations. The shear modulus plots (Figure 10(c) and (d)) show that KGeCl₃ resists deformation more uniformly than KAlCl₃. The Poisson's ratio distribution (Figure 10(e) and (f)) confirms this pattern, supporting the idea that KGeCl₃'s elastic response is more uniform in different directions. Both materials exhibit anisotropy, but KGeCl₃ has a more balanced response.

Based on calculated properties, $KAlCl_3$ and $KGeCl_3$ display direction-dependent behavior, are mechanically stable, and can be deformed without breaking. The higher Young's modulus of $KAlCl_3$ indicates it is stiffer than $KGeCl_3$. The Poisson's ratio supports the idea that the interactions within these materials are mainly ionic. These results enhance our understanding of the mechanical stability and possible uses of $KTCl_3$ (T = Ge or Al) in different technologies.

3.4 Comparison with state-of-the-art materials

To better contextualize our findings, we have compared the properties of $KTCl_3$ (T = Ge, Al) with those of well-known materials used in optoelectronic applications, such as $CsPbBr_3$, $MAPbI_3$, and other relevant chloro-

perovskites. Table 4 summarizes the key properties of these materials, including band gaps, absorption coefficients, and mechanical properties.

KGeCl₃ exhibits a direct band gap of 1.88 eV, which is comparable to CsPbBr₃ (2.30 eV) and MAPbI₃ (1.56 eV), making it suitable for optoelectronic applications. Its high absorption coefficient (187.76 cm⁻¹) indicates strong light absorption, particularly in the UV-visible range, which is advantageous for solar cells and photodetectors. Mechanically, KGeCl₃ shows a bulk modulus of 27.39 GPa and a shear modulus of 28.14 GPa, indicating good mechanical stability and ductility. These properties make KTCl₃ (T = Ge, Al) promising candidates for optoelectronic applications, offering a balance of electronic, optical, and mechanical properties that are competitive with state-of-the-art materials.

4 Conclusion

DFT calculations were performed to investigate the structural, electronic, optical, and elastic properties of KTCl₃ (T = Ge, Al). Both compounds are structurally stable, crystallizing in a cubic phase. Electronic band structure analysis shows that KGeCl₃ is a direct bandgap semiconductor with a gap of 1.88 eV, while KAlCl₃ exhibits metallic behavior due to Al-derived states crossing the Fermi level. The projected DOS reveals that Ge and Cl orbitals dominate the valence and conduction bands in KGeCl₃, whereas Al states primarily contribute to the conduction in KAlCl₃. Optical properties, including the dielectric function, absorption coefficient, reflectivity, and refractive index, indicate strong photon absorption in the UV-visible region, suggesting their applicability in optoelectronic devices such as UV detectors and photonic coatings. The calculated optical conductivity further supports their potential for high-frequency electronic applications. Elastic property analysis confirms mechanical stability and ductility, with the B/G and Poisson's ratios indicating ionic bonding and elastic anisotropy. Although the Tran-Blaha modified

Becke-Johnson (TB-mBJ) potential improves bandgap predictions compared to standard GGA, this study did not employ hybrid functionals such as HSE06, which are

DE GRUYTER

known to provide more accurate electronic and optical descriptions due to the inclusion of non-local exchange. Moreover, excitonic effects were not considered and may influence absorption near the band edge. Despite these limitations, the results provide valuable insights and establish KTCl₃ (T = Ge, Al) as promising candidates for optoelectronic, dielectric, and mechanical device applications.

Acknowledgments: The authors extend their appreciation to the Deanship of Research and Graduate Studies at King Khalid University for funding this research work under the Research Support Program for the Large Group Project at King Khalid University, Kingdom of Saudi Arabia, through the project number RGP2/60/46.

Funding information: This article was funded by Deanship of Research and Graduate Studies at King Khalid University under the Research Support Program for the large group project through the project number RGP2/60/46.

Author contributions: Muhammad Tahir, Wafa Mohammed Almalki, Nasir Rahman, Mudasser Husain, Mohamed Hussien, and Vineet Tirth wrote the manuscript. Khamael M. Abualnaja, Abid Ali Khan, Amir Ullah, Rajwali Khan, and Aurangzeb Khan prepared the figures. All authors have accepted responsibility for the entire content of this manuscript and approved its submission.

Conflict of interest: The authors state no conflict of interest.

Data availability statement: The datasets generated and/ or analyzed during the current study are available from the corresponding author on reasonable request.

References

- Khalid S, Fahad S, Khan J, Sun X, Khenata R, Huang W, et al. Understanding the structural, electronic and optical properties of CuXY2 (X = Si, Ge, Y = P, As): A DFT + U approach. Optik (Stuttg).
- Ullah A, Rahman N, Husain M, Almalki WM, Hussien M, Tirth V, et al. DFT study of structural, elastic and optoelectronic properties of binary X2Se (X = Cd, Zn) chalcogenides. Inorg Chem Commun. 2025;174:113985.
- Roknuzzaman M, Alarco JA, Wang H, Du A, Tesfamichael T, Ostrikov KK. Ab initio atomistic insights into lead-free

- formamidinium based hybrid perovskites for photovoltaics and optoelectronics. Comput Mater Sci. 2019;169:109118.
- Roknuzzaman M, Ostrikov KK, Wasalathilake KC, Yan C, Wang H, [4] Tesfamichael T. Insight into lead-free organic-inorganic hybrid perovskites for photovoltaics and optoelectronics: A first-principles study. Org Electron. 2018;59:99-106.
- Tseng Y-T, Wu CC. Photovoltaic performance of CH₃NH₃PbI₂Cl perovskite solar cell. Appl Funct Mater. 2022;2(2):4-20.
- Murtaza G, Ahmad I. First principle study of the structural and [6] optoelectronic properties of cubic perovskites CsPbM₃ (M=Cl, Br, I) . Phys B: Condens Matte. 201;17(1):3222-9.
- Korba SA, Meradji H, Ghemid S, Bouhafs B. First principles calculations of structural, electronic and optical properties of BaLiF3. Comput Mater Sci. 2009:44(4):1265-71.
- Boumriche A, Gesland JY, Bulou A, Rousseau M, Fourquet JL, Hennion B. Structure and dynamics of the inverted perovskite BaLiF3. Solid State Commun. 1994;91(2):125-8.
- [9] Sarhani ME, Dahame T, Belkhir ML, Bentria B, Begagra A. AB-INITIO study of electronic, mechanical, optical and thermoelectric properties of KGeCl3 for photovoltaic application. Heliyon. 2023;9(9):e19808.
- Tarekuzzaman M, Ishrag MH, Parves MS, Rayhan MA, Ahmad S, Rasheduzzaman M, et al. An in-depth investigation of lead-free KGeCl 3 perovskite solar cells employing optoelectronic, thermomechanical, and photovoltaic properties: DFT and SCAPS-1D frameworks. Phys Chem Chem Phys. 2024;26(43):27704-34.
- Islam MR, Mojumder MRH, Islam ASMJ, Alom MZ. Strain-driven tunability of the optical, electronic, and mechanical properties of lead-free inorganic CsGeCl3 perovskites. Phys Scr. 2022;97(12):125817.
- Hao F, Stoumpos CC, Cao DH, Chang RPH, Kanatzidis MG. Lead-free [12] solid-state organic-inorganic halide perovskite solar cells. Nat Photonics. 2014;8(6):489-94.
- Jithin PV, Bitla Y, Patidar MM, Ganesan V, Sankaran KJ, Kurian J. Enhanced magnetoresistance and evolution of Griffiths-like phase in La_{1-x} Ca_x MnO₃ (x = 0.4, 0.5) nanoparticles. J Nanopart Res. 2023;25(10):207.
- Mubarak AA, Mousa AA. The electronic and optical properties of the fluoroperovskite BaXF3 (X = Li, Na, K, and Rb) compounds. Comput Mater Sci. 2012;59:6-13.
- [15] Mousa AA, Mahmoud NT, Khalifeh JM. The electronic and optical properties of the fluoroperovskite XLiF3 (X = Ca, Sr, and Ba) compounds. Comput Mater Sci. 2013;79:201-5.
- [16] Yalcin BG, Salmankurt B, Duman S. Investigation of structural, mechanical, electronic, optical, and dynamical properties of cubic BaLiF3, BaLiH3, and SrLiH3. Mater Res Express. 2016;3(3):36301.
- Suchikova Y, Kovachov S, Bohdanov I, Karipbayev ZT, Zhydachevskyy Y, Lysak A, et al. Advanced synthesis and characterization of CdO/CdS/ZnO heterostructures for solar energy applications. Materials (Basel). 2024;17(7):1566.
- Chowdhury N, Riesen N, Riesen H. Efficient generation of stable Sm2+ in nanocrystalline BaLiF3: Sm3+ by UV-and X-irradiation. J Phys Chem C. 2019;123(41):25477-81.
- Pingak RK, Bouhmaidi S, Setti L. Investigation of structural, electronic, elastic and optical properties of Ge-halide perovskites NaGeX3 (X = Cl, Br and I): A first-principles DFT study. Phys B Condens Matter. 2023;663:415003.
- Lynn MO, Ologunagba D, Dangi BB, Kattel S. Density functional theory study of bulk properties of transition metal nitrides. Phys Chem Chem Phys. 2023;25(6):5156-63.

- [21] Sholihun S, Kadarisman HP, Nurwantoro P. Density-functionaltheory calculations of formation energy of the nitrogen-doped diamond. Indones J Chem. 2018;18(4):749–54.
- [22] Azam S, Goumri-Said S, Khan SA, Kanoun MB. Electronic, optical and thermoelectric properties of new metal-rich homological selenides with palladium-indium: Density functional theory and Boltzmann transport model. J Phys Chem Solids. 2020;138:109229.
- [23] Hutama AS, Huang H, Kurniawan YS. Investigation of the chemical and optical properties of halogen-substituted N-methyl-4-piperidone curcumin analogs by density functional theory calculations. Spectrochim Acta Part A Mol Biomol Spectrosc. 2019;221:117152.
- [24] Hauwali NUJ, Syuhada I, Rosikhin A, Winata T. Fundamental properties of parallelogram graphene nanoflakes: A first principle study. Mater Today Proc. 2021;44:3305–8.
- [25] Pradipta MF, Pranowo HD, Alfiyah V, Hutama AS. Theoretical study of oxygen atom adsorption on a polycyclic aromatic hydrocarbon using density-functional theory. Indones J Chem. 2021;21(5):1072–85.
- [26] Jena AK, Kulkarni A, Miyasaka T. Halide perovskite photovoltaics: Background, status, and future prospects. Chem Rev. 2019;119(5):3036–103.
- [27] Mubarak AA, Al-Omari S. First-principles calculations of two cubic fluoropervskite compounds: RbFeF3 and RbNiF3. J Magn Magn Mater. 2015;382:211–8.
- [28] Ahmad R, Mehmood N. A density functional theory investigations of half-heusler compounds RhVZ (Z = P, As, Sb). J Supercond Nov Magn. 2018;31(5):1577–86.
- [29] Khan NU, Abdullah N, Khan UA, Tirth V, Al-Humaidi JY, Refat MS, et al. Investigation of structural, opto-electronic and thermoelectric properties of titanium based chloro-perovskites XTiCl3 (X = Rb, Cs): A first-principles calculations. RSC Adv. 2023 Feb;13(9):6199–209.
- [30] Azeem W, Shahzad MK, Wong YH, Tahir MB. Ab-initio calculations for the study of the hydrogen storage properties of CsXH3 (X = Co, Zn) perovskite-type hydrides. Int J Hydrog Energy. 2024;50:305–13.
- [31] Khan I, Ullah A, Rahman N, Husain M, Tirth V, Sohail M. First principle study of structural and optoelectronic properties of ZnLiX3 (X = Cl or F) perovskites. Results Phys. 2024;66:108019.
- [32] Pei Z, Leng K, Xia W, Lu Y, Wu H, Zhu X. Structural characterization, dielectric, magnetic and optical properties of double perovskite Bi2FeMnO6 ceramics. J Magn Magn Mater. 2020;508:166891.
- [33] Kim H, Han JS, Choi J, Kim SY, Jang HW. Halide perovskites for applications beyond photovoltaics. Small Methods. 2018;2(3): 1700310.
- [34] Rahman N, Husain M, Yang J, Sajjad M, Murtaza G, Ul Haq M, et al. First principle study of structural, electronic, optical and mechanical properties of cubic fluoro-perovskites:(CdXF3, X = Y, Bi). Eur Phys J Plus. 2021;136(3):1–11.
- [35] van Blaaderen JJ, van den Brekel LA, Krämer KW, Dorenbos P. Scintillation and Optical Characterization of CsCu2I3 Single Crystals from 10 to 400 K. Chem Mater. 2023;35(22):9623–31.
- [36] Mandal S, Sarkar P. Physical insights into the ultralow lattice thermal conductivity and high thermoelectric performance of bulk LiMTe 2 (M = Al, Ga). J Mater Chem C. 2023;11(40):13691–706.

- [37] Chaba Mouna S, Radjai M, Bouhemadou A, Rahman MA, Kara H, Houatis D, et al. Structural, electronic, and optical characteristics of BaXCl3 (X = Li, Na) perovskites. Mater Sci Eng B. 2024;308:117578.
- [38] Mubarak AA. Ab initio study of the structural, electronic and optical properties of the fluoropervskite SrXF3 (X = Li, Na, K and Rb) compounds. Comput Mater Sci. 2014;81:478–82.
- [39] Ephraim Babu K, Murali N, Vijaya Babu K, Taddesse Shibeshi P, Veeraiah V. Structural, elastic, electronic, and optical properties of cubic perovskite CsCaCl₃ compound: An ab initio study. Acta Phys Pol A. 2014;125(5):1179–85.
- [40] Arjun U, Ranjith KM, Jesche A, Hirschberger F, Sarma DD, Gegenwart P. Efficient adiabatic demagnetization refrigeration to below 50 mK with Ultrahigh-Vacuum-Compatible Ytterbium Diphosphates A YbP 2 O 7 (A = Na, K). Phys Rev Appl. 2023;20(1):14013.
- [41] Ullah W, Nasir R, Husain M, Rahman N, Ullah H, Sfina N, et al. Revealing the remarkable structural, electronic, elastic, and optical properties of Zn-based fluoropervskite ZnXF3 (x = Sr, Ba) employing DFT. Indian | Phys. 2024;1–12.
- [42] Jamal M, Bilal M, Ahmad I, Jalali-Asadabadi S. IRelast package. J Alloy Compd. 2018;735:569–79.
- [43] Husain M, Ahmad MS, Rahman N, Sajjad M, Rauf A, Habib A, et al. First principle study of the structural, electronic, and mechanical properties of cubic fluoroperovskites: (ZnXF 3, X = Y, Bi). Fluoride. 2020;53(4):657–67.
- [44] Pitriana P, Wungu TDK, Hidayat R. The characteristics of band structures and crystal binding in all-inorganic perovskite APbBr3 studied by the first principle calculations using the Density Functional Theory (DFT) method. Results Phys. 2019:15:102592.
- [45] Ullah A, Rahman N, Husain M, Abualnaja KM, Alosaimi G, Belhachi S, et al. Unlocking the physical properties of RbXBr3 (X = Ba, Be) halide perovskites for potential applications: DFT study. Inorg Chem Commun. 2025;173:113879.
- [46] Harmel M, Khachai H, Haddou A, Khenata R, Murtaza G, Abbar B, et al. Ab initio study of the mechanical, thermal and optoelectronic properties of the cubic CsBaF₃. Acta Phys Pol A. 2015;128(1):34–42.
- [47] Johannes AZ. Simulasi Perubahan Densitas Muatan Adsorpsi Atom Hidrogen-Grafena Dengan Teori Fungsi Kerapatan. J Fis Fis Sains Dan Apl. 2018;3(2):179–84.
- [48] Ezzeldien M, Al-Qaisi S, Alrowaili ZA, Alzaid M, Maskar E, Es-Smairi A, et al. Electronic and optical properties of bulk and surface of CsPbBr3 inorganic halide perovskite a first principles DFT 1/2 approach. Sci Rep. 2021;11(1):20622.
- [49] Rahman TB, Rahman MM, Amir-Al Zumahi SM, Islam MR, Rahman MM. Strain-tuned structural, optoelectronic and dielectric properties of cubic MAPbI3 perovskite driven by SOC using firstprinciples theory. Solid State Commun. 2024;394:115728.
- [50] El Akkel M, Dahbi S, Benyoussef S, Tahiri N, Ez-Zahraouy H. First-principles studies of structural, vibrational, elastic, optoelectronic, and thermoelectric properties of doped, alloyed, and strained CsGeCl3 for photovoltaic applications. Sol Energy. 2024;282:112903.